

Searches for LFV at B factories

K Hayasaka

Nagoya University, Furo-cho, Chikusa-ku, Nagoya, Japan

E-mail: hayasaka@hepl.phys.nagoya-u.ac.jp

Abstract. Lepton-flavor violating (LFV) decay in τ , B and $\Upsilon(nS)$ is expected to be very small in the Standard Model, even taking into account the effect of neutrino mixing. Therefore, the observation of such decays would be a clear signal of new physics. The production rate of τ pairs at B factory is comparable to that of B meson pairs and hence B factories are also excellent τ factories. Many LFV decay modes have been searched for at the B factories. We present the current status of searches for tau LFV decays as well as B and $\Upsilon(nS)$ LFV decays. Some of the upper limits are now reaching to a range predicted by some new physics models.

1. Introduction

In the Standard Model (SM), only lepton-flavor conserving processes are allowed. On the other hand, various scenarios for the extension of SM or New Physics (NP) naturally include some LFV processes. However, in the SM with neutrino oscillations, for example, the branching fractions of $\tau \rightarrow \mu\gamma$ and $\tau \rightarrow \mu\mu\mu$ are extremely small, i.e., $\mathcal{O}(10^{-49\sim-52})$ and $\mathcal{O}(10^{-14})$, respectively [1]. It makes their experimental observation impossible.

Since many NP models, such as SUSY models, predict that the various charged LFV processes are enhanced significantly, an observation of such a process is a clear signal of NP. Among them, τ lepton has more than 40 possible LFV decay modes because it is the heaviest lepton and can into various hadrons. According to the most optimistic prediction, at least, we need the sensitivity of $\mathcal{O}(10^{-7})$ for the branching fraction to observe the τ LFV decays, experimentally. (See Table 1.)

Table 1. Theoretical predictions of the possibly largest branching fraction of $\tau \rightarrow \mu\gamma$ and $\tau \rightarrow \mu\mu\mu$ modes

Model	$\mathcal{B}(\tau \rightarrow \mu\gamma)$	$\mathcal{B}(\tau \rightarrow \mu\mu\mu)$	Ref.
SM + ν mixing	10^{-49-52}	10^{-14}	[1]
SM + heavy Majorana ν_R	10^{-9}	10^{-10}	[2]
Non-universal Z'	10^{-9}	10^{-8}	[3]
SUSY SO(10)	10^{-8}	10^{-10}	[4]
mSUGRA + seesaw	10^{-7}	10^{-9}	[5]
SUSY higgs	10^{-10}	10^{-7}	[6]

To discriminate models, search for various LFV modes is helpful; while many NP models predict that the branching fraction for $\tau \rightarrow \mu\gamma$ should be largest, the Higgs-mediated model [7] enhances $\tau \rightarrow \mu\eta$ via the neutral Higgs ($h/H/A$) when the sleptons are much heavier than the weak scale.¹ The ratios between theoretically predicted branching fractions of $\tau \rightarrow \mu\gamma$, $\tau \rightarrow \mu\mu\mu$, and $\tau \rightarrow \mu ee$ are summarized in Table 2.

Table 2. Ratios between the branching fractions of $\tau \rightarrow \mu\gamma$, $\tau \rightarrow \mu\mu\mu$, and $\tau \rightarrow \mu ee$ in various NP models, based on [9].

	SUSY+GUT (SUSY+Seesaw)	Higgs mediated	Little Higgs	Non-universal Z' boson
$\frac{\mathcal{B}(\tau \rightarrow \mu\mu\mu)}{\mathcal{B}(\tau \rightarrow \mu\gamma)}$	$\sim 2 \times 10^{-3}$	~ 0.1	$0.4 \sim 2.3$	20
$\frac{\mathcal{B}(\tau \rightarrow \mu ee)}{\mathcal{B}(\tau \rightarrow \mu\gamma)}$	$\sim 1 \times 10^{-2}$	$\sim 1 \times 10^{-2}$	$0.3 \sim 1.6$	~ 20
$\mathcal{B}(\tau \rightarrow \mu\mu\mu)$	$< 10^{-7}$	$< 10^{-10}$	$< 10^{-10}$	$< 10^{-9}$

2. KEKB/Belle and PEP-II/BaBar

The KEKB is a e^+e^- asymmetric-energy collider operating at the center-of-mass (CM) energy corresponding to the $\Upsilon(4S)$ resonance. Experiments at the KEKB allow searches for LFV decays with a very high sensitivity since the cross section of $\tau^+\tau^-$ production is $\sigma_{\tau\tau} \simeq 0.9$ nb, close to that of $B\bar{B}$ production, $\sigma_{B\bar{B}} \simeq 1$ nb, and thus, B -factories are also excellent τ -factories. By summer 2008, the Belle detector [10] operating at the KEKB B -factory [11] accumulated about 7.8×10^8 τ pairs. Belle detector is the multi-purpose detector which has good track reconstruction and particle identification ability.

Similarly, the BABAR detector, described in more detail elsewhere [12], collects data at the PEP-II asymmetric-energy e^+e^- collider that operates at a CM energy of 10.58 GeV. Finally, a 557 fb^{-1} data sample has been accumulated before the PEP-II collider stops running

3. Method

All searches for LFV τ decays follow a similar procedure. We search for $\tau^+\tau^-$ events in which one τ (signal side) decays into an LFV mode under study, while the other τ (tag side) decays into one (or three) charged particles and any number of additional photons and neutrinos (for example, see Fig. 1 (a)). To search for exclusive LFV-decay modes, we select low multiplicity events with zero net charge, and separate an event into two hemispheres (signal and tag) using a thrust axis. The backgrounds in such searches are dominated by $q\bar{q}$ ($q = u, d, s, c$), generic $\tau^+\tau^-$, two-photon, $\mu^+\mu^-$ and Bhabha events. To obtain the good sensitivity, we optimize the event selection using particle identification and kinematic information for each mode separately. Because every τ LFV decay is a neutrinoless one, the information from missing tracks is very powerful to reject the background from generic $\tau^+\tau^-$ events. As an example, our typical event selection uses the relation between the missing momentum p_{miss} and missing mass squared m_{miss}^2 since neutrinos are included in the tag side only in a signal event (see Figures 1 (b) and (c)).

After signal selection criteria are applied, signal candidates are examined in the two-dimensional space of the invariant mass, M_{inv} , and the difference of their energy from the

¹ Recently, detailed estimations concerning this model were discussed in [8].

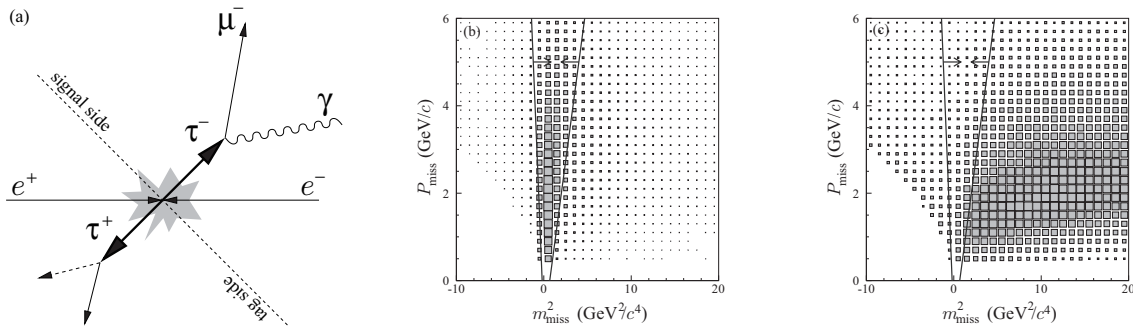


Figure 1. Event topology of LFV τ decay in case of $\tau \rightarrow \mu\gamma$ analysis (a), Scatter-plots of p_{miss} vs. m_{miss}^2 for the $\tau^- \rightarrow \mu^- \gamma$ signal Monte Carlo (MC) (b) and the generic $\tau^+ \tau^-$ MC (c) distributions.

beam energy in the CM system, ΔE . A signal event should have M_{inv} close to the τ -lepton mass and ΔE close to 0. Generally, Belle often uses M_{inv} , while BaBar prefers instead a beam-energy-constrained mass, M_{bc} , where the reconstructed τ energy must be equal to the beam energy in the CM frame. We blind a region around the signal region in the $M_{\text{inv}} - \Delta E$ plane so as not to bias our choice of selection criteria. The expected number of background events in the blind region is first evaluated, and then the blind region is opened and candidate events are counted. By comparing the expected and observed numbers of events, we either observe a LFV τ decay or set an upper limit by applying counting [13] or maximum likelihood [14] approaches.

4. Results

4.1. $\tau^- \rightarrow \ell^- \gamma$

Figure 2 (a) shows scatter-plots in the $M_{\text{inv}} - \Delta E$ plane for the $\tau^- \rightarrow \mu^- \gamma$ mode, obtained after event selection at Belle using 535 fb^{-1} of data. The dominant background for this mode comes from generic $\tau\tau$ events where one τ decays into $\ell\nu\bar{\nu}$ with initial state radiation. In order to evaluate the number of signal events, an unbinned extended maximum likelihood fit is applied. Consequently, -3.9 (-0.14) events for the number of signal and 13.9 (5.14) for the number of background events are evaluated in the $\tau \rightarrow \mu\gamma$ ($e\gamma$) modes. From these results, the following upper limits for the branching fraction at the 90% confidence level are set: $\mathcal{B}(\tau^- \rightarrow \mu^- \gamma) < 4.5 \times 10^{-8}$ and $\mathcal{B}(\tau^- \rightarrow e^- \gamma) < 1.2 \times 10^{-7}$ [15]. The sensitivity is limited by the background from $\tau^+ \tau^-$ events with initial state radiation.

BaBar also searches the signal of $\tau \rightarrow \mu\gamma/e\gamma$ with a 211 fb^{-1} data sample. After event selection, the remaining data distribution is shown in Fig. 2 (b). By the maximum likelihood fit, the number of signal events is evaluated to be -2.2 for $\tau \rightarrow \mu\gamma$ and the 90% confidence level upper limit is derived to be 6.8×10^{-8} [16]. For $\tau \rightarrow e\gamma$ analysis, the counting method is taken to evaluate the number of signal events. After event selection, one event is found and its upper limit on the branching fraction is set to be 1.1×10^{-7} at 90% confidence level [17].

Hereafter, upper limits for τ decays are evaluated by the counting method.

4.2. $\tau^- \rightarrow \ell^- \eta, \ell^- \eta', \ell^- \pi^0$

Belle searches for lepton-flavor-violating τ decays with a pseudoscalar meson (η, η' and π^0) using 401 fb^{-1} of data. No signal is found and the following upper limits on branching fractions are set as $(6.5 - 12) \times 10^{-8}$ at the 90% confidence level [18].

BaBar also performs the analysis for these modes with a 339 fb^{-1} data sample [19]. The number of observed events is 0 or 1 and the evaluated upper limits on the branching fraction

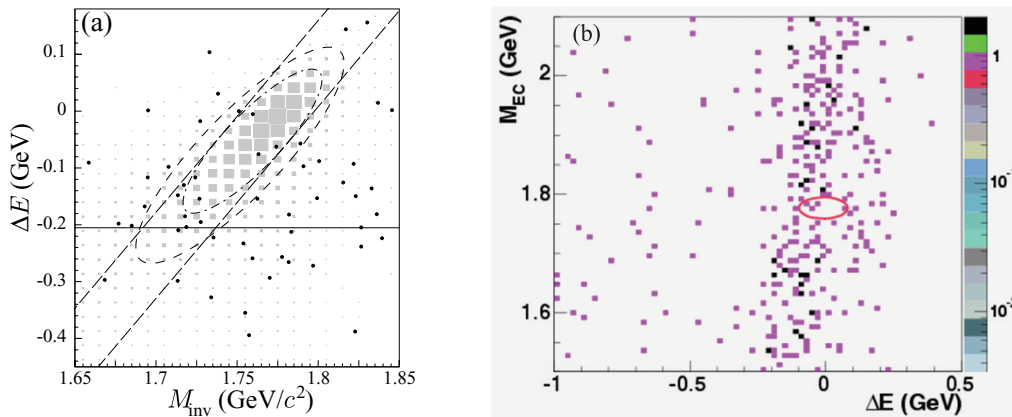


Figure 2. Scatter-plots in the $M_{\text{inv}} - \Delta E$ plane by Belle (a) and BaBar (b): In (a), the data are indicated by the solid circles. The filled boxes show the MC signal distribution with arbitrary normalization. The large elliptical regions shown are used for evaluating the blind yield while the small elliptical regions shown are used for evaluating the signal yield. In (b), M_{bc} is taken instead of M_{inv} and the vertical and horizontal axes are exchanged against (a). Here, the data distribution is shown with colored box. The elliptic region corresponds to 2σ signal region.

are $(11 - 26) \times 10^{-8}$ at 90% confidence level.

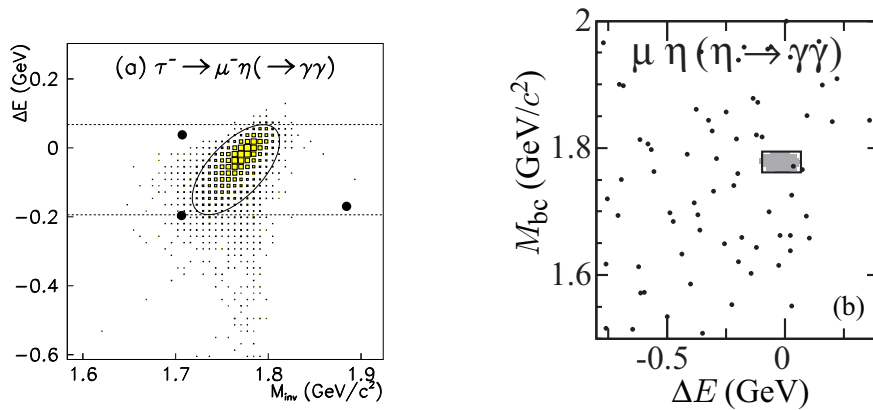


Figure 3. Scatter-plots in the $M_{\text{inv}} - \Delta E$ plane for $\tau \rightarrow \mu\eta$ with $\eta \rightarrow \gamma\gamma$ analysis by Belle (a) and BaBar (b): In (a), the data and signal MC distribution are expressed by black dots and yellow boxes, respectively. The signal region is defined by the elliptic region which includes 90% of remaining signal events. In (b), the dots (shaded boxes) correspond to the data (signal) distribution. The small box is a 2σ signal region.

4.3. $\tau^- \rightarrow \ell^- \ell^+ \ell^-$

The following τ^- decays into three leptons are considered: $e^- e^+ e^-$, $\mu^- \mu^+ \mu^-$, $e^- \mu^+ \mu^-$, $\mu^- e^+ e^-$, $\mu^- e^+ \mu^-$ and $e^- \mu^+ e^-$. Experimentally, these modes can be separated well from the background due to the good lepton identification and track reconstruction.

Recently, Belle updated this result with 535 fb^{-1} of data [20]. Since each decay mode has different background, the event selection is optimized mode by mode. The signal efficiencies

are kept in the range of (6.0-12.5)%. After event selection, no events are observed in the signal region for all modes while the expected background is less than 0.4 events as shown in Fig. 4. Therefore, no evidence for these decays is observed and 90% confidence level upper limits on the branching fractions are set to be $(2.0-4.1) \times 10^{-8}$. The branching fraction of $\tau^- \rightarrow \mu^+ e^- e^-$ is the most stringent upper limit ($< 2.0 \times 10^{-8}$) among currently measured LFV τ decays.

Similarly, BaBar also updated this result with 339 fb^{-1} of data [21]. The number of observed events is (0 – 2) while the expected number of BG is (0.30 – 1.33) with the detection efficiency of (5.5 – 12.4)%. As a result, the 90% uppler limits on the branching fractions are evaluated to be $(3.7 – 8.0) \times 10^{-8}$.

The background for these decays are negligible both Belle and BaBar experiments.

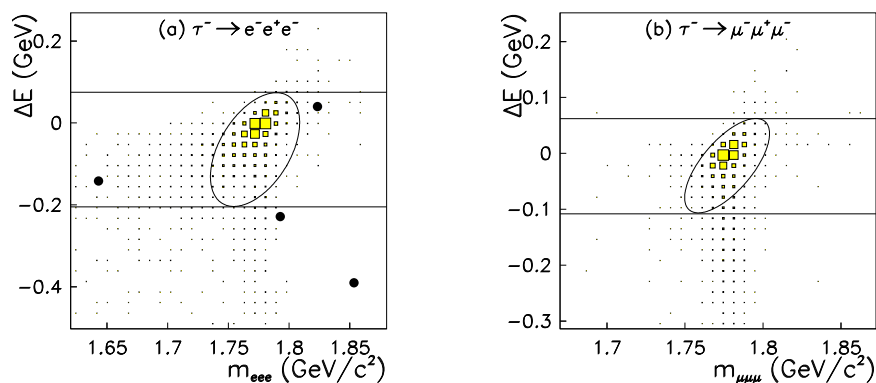


Figure 4. Scatter-plots for $\tau \rightarrow eee$ (a) and $\tau \rightarrow \mu\mu\mu$ (b) by Belle. In both of them, the signal distribution is expressed by yellow boxes and the data is indicated by the black dots.

4.4. $\tau^- \rightarrow \ell^- f_0(980)$

Belle searches for LFV τ decays into a lepton (electron or muon) and an $f_0(980)$ meson using 671 fb^{-1} of data [22]. In this analysis, the $f_0(980) \rightarrow \pi^+ \pi^-$ decay mode is taken and it is required that the invariant mass satisfy the condition $906 \text{ MeV}/c^2 < M_{\pi^+ \pi^-} < 1065 \text{ MeV}/c^2$ for $f_0(980)$ selection. Figure 5 shows scatter-plots for the data and the signal MC distributed over $\pm 20\sigma$ in the $M_{\text{inv}} - \Delta E$ plane after the event selection. The expected numbers of background in the signal region are around 0.1 events for both modes and no events are observed. Finally, the following 90% C.L. upper limits on the branching fraction products are set: $\mathcal{B}(\tau^- \rightarrow e^- f_0(980)) \times \mathcal{B}(f_0(980) \rightarrow \pi^+ \pi^-) < 3.2 \times 10^{-8}$ and $\mathcal{B}(\tau^- \rightarrow \mu^- f_0(980)) \times \mathcal{B}(f_0(980) \rightarrow \pi^+ \pi^-) < 3.4 \times 10^{-8}$. This is the first search performed for these modes.

4.5. $\tau^- \rightarrow \ell^- V^0$

Belle recently updated their searches, $\tau^- \rightarrow \ell^- V^0$ where V^0 is a neutral vector mesons such as ρ^0 , ϕ , $K^*(892)^0$, $\bar{K}^*(892)^0$ and ω , based on a data sample of 543 fb^{-1} of data [23].

The main background is SM τ decays, such as $\tau \rightarrow \pi \omega \nu$ and $\tau \rightarrow 3 \pi \nu$. No excesses are observed and upper limits on the branching fractions are set in the range $(0.6 - 1.8) \times 10^{-7}$ at the 90% confidence level.

BaBar separately reports the result for $\tau^- \rightarrow \ell^- \omega$ with a 384 fb^{-1} data sample [24] and the others with a 451 fb^{-1} data sample [25], where the result of the latter is preliminary. The $\Delta M - \Delta E$ scatter-plots of the latter one after event selection are shown in Fig. 6, where ΔM is defined as $M_{bc} - m_\tau$.

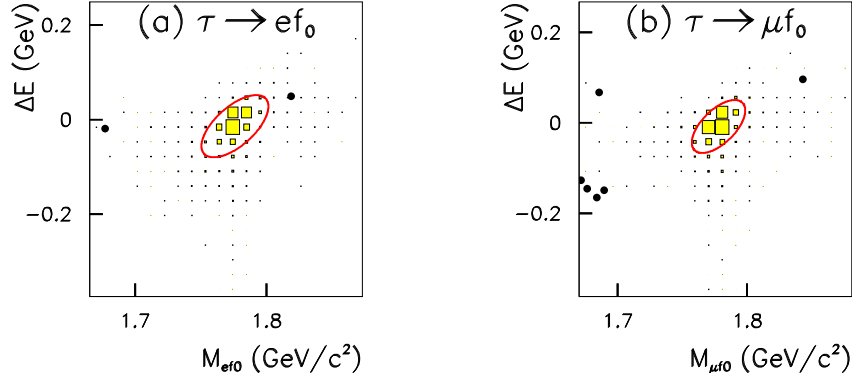


Figure 5. Scatter-plots in the $M_{\text{inv}} - \Delta E$ plane: (a) and (b) correspond to the $\pm 20\sigma$ area for the $\tau^- \rightarrow e f_0(980)$ and $\tau^- \rightarrow \mu^- f_0(980)$ modes, respectively. The data are indicated by the solid circles. The yellow boxes show the MC signal distribution with arbitrary normalization. The elliptical signal regions shown by a solid curve are used for evaluating the signal yield.

As a result, the 90% confidence level upper limits on the branching ratio of $(0.8 - 18) \times 10^{-8}$ are obtained.

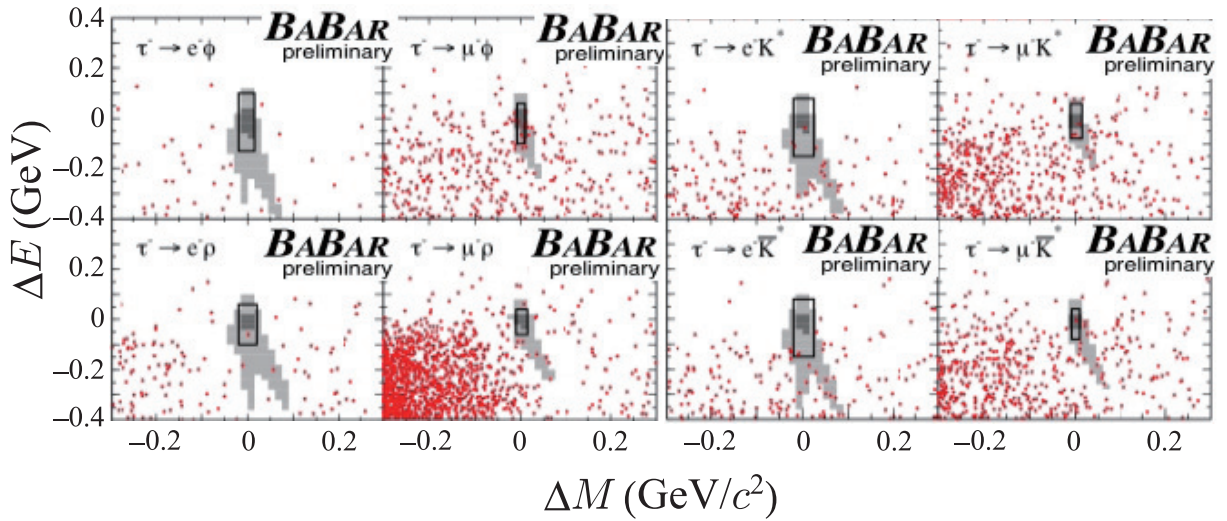


Figure 6. Scatter-plots in the $\Delta M - \Delta E$ plane obtained by BaBar, where $\Delta M \equiv M_{\text{bc}} - m_\tau$. In each plot, shaded (colored) boxes mean the signal MC (data) distribution and the black rectangle is a signal region.

4.6. $B^0 \rightarrow e^\pm \mu^\mp$

From here, we discuss the LFV processes other than τ decays.

Some NP models predict that the branching fraction on $B^0 \rightarrow e^\pm \mu^\mp$ can be up to $10^{-10 \sim -16}$.

BaBar searches for this decay with $3.8 \times 10^6 B\bar{B}$ pairs [26]. Similarly to τ LFV analysis, in this decay, B^0 can be completely reconstructed from e and μ . Therefore, to evaluate the

number of signal events, $M_{\text{inv}} - \Delta E$ plane is effective and the signal region is defined there. The main $B\bar{B}$ BG comes from $B^0 \rightarrow \pi\pi, \pi K$ where the hadron is misidentified as a lepton. By the maximal likelihood fit, the number of signal events is evaluated to be 1.1 and the upper limit on the branching fraction is set to be 9.2×10^{-8} at 90% confidence level.

4.7. $B^0 \rightarrow \ell^\pm \tau^\mp$

In the Higgs-mediated model, the branching fraction on $B^0 \rightarrow \ell^\pm \tau^\mp$ can be enhanced up to 2×10^{-10} .

This decay is searched for by BaBar with $3.8 \times 10^6 B\bar{B}$ pairs [27]. In this analysis, differently from the $B^0 \rightarrow e^\pm \mu^\mp$ case, it is difficult to reconstruct the signal B (B_{sig}) due to existence of τ in the final state. Therefore, one B (B_{tag}) is fully reconstructed in the specific hadronic mode ($B \rightarrow D^{(*)} X_{\text{had}}$, where X_{had} is a combination of up to nine neutral/charged kaons and pions). And then, in the rest of the event, the $\ell^\pm \tau^\mp$ signature is searched for to find the B_{sig} where six τ decay modes are considered: $\tau \rightarrow e\nu\nu, \mu\nu\nu, \pi\nu, \pi\pi^0\nu, \pi 2\pi^0\nu, 3\pi\nu$. The signal yield is extracted from a maximum likelihood fit to the signal lepton candidate momentum distribution in the B_{sig} rest frame and 0.02/9.35 (0.01/13.03) signal/BG events are obtained in the $B^0 \rightarrow e^\pm \tau^\mp$ ($B^0 \rightarrow \mu^\pm \tau^\mp$) analysis. Finally, the 90% confidence level upper limit on the branching fraction for $B^0 \rightarrow e^\pm \tau^\mp$ ($B^0 \rightarrow \mu^\pm \tau^\mp$) is evaluated to be $2.8(2.2) \times 10^{-5}$.

4.8. $B^+ \rightarrow K^+ \mu^\pm \tau^\mp$

The semileptonic decay $B^+ \rightarrow K^+ \mu^\pm \tau^\mp$ is expected to have higher sensitivity to NP, in comparison with leptonic decays such as $B^0 \rightarrow \mu\tau$, since the latter is both helicity and Cabibbo-Kobayashi-Maskawa quark-mixing matrix suppressed by a factor of $|V_{td}/V_{cb}|^2$.

BaBar searched for this decay with $3.8 \times 10^6 B\bar{B}$ pairs [28]. In the same way in the previous section, the full reconstruction method is applied for B_{tag} . After requiring exactly three charged tracks in the event not associated with B_{tag} , those are candidates for K, μ and a daughter of τ , are selected, the 4-momentum of τ is completely determined from B_{sig}, K and μ when the momentum of B_{sig} in the CM frame is evaluated as $-p$ of B_{tag} . The dominant BG comes from $B \rightarrow (c\bar{c})K$ with $(c\bar{c}) \rightarrow \mu\mu$, where $(c\bar{c})$ is a charmonium resonance. The signal extraction is performed on the reconstructed τ mass distribution and its upper limit is evaluated in the counting method. Finally, the upper limit on the branching fraction is set to be 7.7×10^{-5} at 90% confidence level.

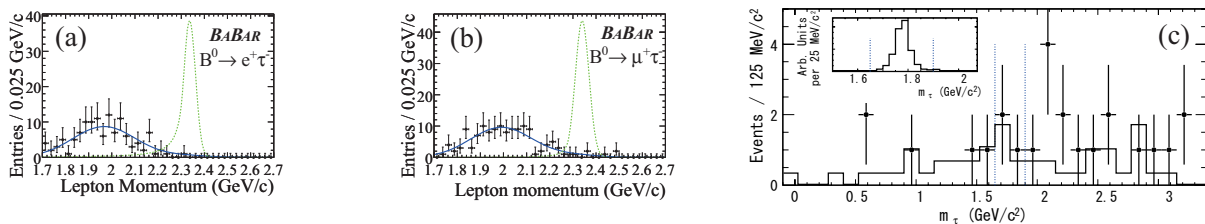


Figure 7. Distributions to extract the signal yield for $B^0 \rightarrow e^+ \tau^-$ (a), $B^0 \rightarrow \mu^+ \tau^-$ (b) and $B^+ \rightarrow K^+ \mu^+ \tau^-$ (c). In (a) and (b), the distribution of the electron and muon momentum are used, respectively. Here, the green line represents the signal PDF with an arbitrary normalization, the blue line shows the background shape and the dots are data. In (c), distribution of m_τ is taken and applied for the data (points with error bars), background Monte Carlo sample (main histogram), and signal Monte Carlo sample (inset histogram). The dotted vertical lines show the m_τ signal region [1.65, 1.90] GeV/c².

4.9. $\Upsilon(nS) \rightarrow \mu^\pm \tau^\mp$ ($n = 1, 2, 3$)

Here, we discuss LFV bottomonium decays $\Upsilon(nS) \rightarrow \mu^\pm \tau^\mp$ ($n = 1, 2, 3$). Various NP models predict such decays via the flavor-changing neutral currents with, e.g., R -parity violating and large $\tan\beta$ SUSY scenarios, leptoquarks and so on.

Recently, CLEO searched for these decays with 20.8, 9.3 and 5.9 million $\Upsilon(1S)$, $\Upsilon(2S)$ and $\Upsilon(3S)$ resonance data samples, respectively [29]. The signature of the signal events is a muon and an electron from the τ decay and the signal events are extracted on the $x - y$ plane, where $x \equiv p_\mu/E_{\text{beam}}$ and $y \equiv p_e/E_{\text{beam}}$. After the selection, by a maximum likelihood method, the number of the signal and BG events is evaluated and the 95% confidence level upper limits on the branching fraction for $\Upsilon(1S) \rightarrow \mu^\pm \tau^\mp$, $\Upsilon(2S) \rightarrow \mu^\pm \tau^\mp$ and $\Upsilon(3S) \rightarrow \mu^\pm \tau^\mp$ are set to be 6.0, 14.4 and 20.3×10^{-6} , respectively.

5. Future Prospect

LFV sensitivity depends on the remaining background level. For the $\tau \rightarrow \mu\gamma$ mode, there is large remaining background from $\tau^+ \tau^-$ events with initial state radiation. In this case, the sensitivity for $\tau \rightarrow \mu\gamma$ is scaled as $1/\sqrt{\mathcal{L}}$ where \mathcal{L} means a luminosity. On the other hand, the remaining background events for the $\tau \rightarrow \ell\ell\ell'$ and ℓ +meson modes are expected to be negligible even for 50 times larger data set, i.e., at 50 ab^{-1} . Therefore, the accessible branching fractions of these modes scale linearly with luminosity from the current upper limits. A Super B -factory is planned to collect more than 50-times larger luminosity than the current one. Therefore, the accessible branching fraction of $\tau \rightarrow \mu\gamma$ at the Super B -factory is $O(10^{-8\sim-9})$ while the accessible branching fractions of $\tau \rightarrow \ell\ell\ell$ and ℓ +meson are $O(10^{-9\sim-10})$ as shown in Fig. 8. Also, in LHC, $\tau \rightarrow \mu\mu\mu$ will be investigated. However, the sensitivity of the super B -factory is 10 times better than that of LHC. Thus, we conclude that the super B -factory will provide us valuable information for various NP scenarios.

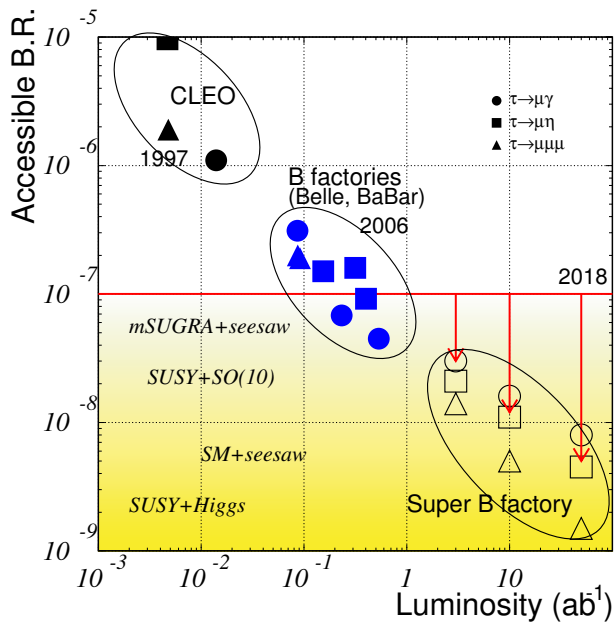


Figure 8. Accessible branching fraction of LFV decay as a function of the integrated luminosity.

6. Summary

We have searched for 46 major modes of lepton flavor violating τ decays with $O(10^9)$ $\tau^+ \tau^-$ pairs data collected by the Belle detector at the KEKB asymmetric-energy $e^+ e^-$ collider and the BaBar detector at the PEP-II asymmetric-energy $e^+ e^-$ collider. The current status of the

τ -LFV searches in B -factory experiments are summarized in Table 3. No evidence for these decays is observed and we set 90% confidence level upper limits on the branching fractions at the $O(10^{-8})$ level. The sensitivity for the LFV search is 100 times improved in comparison with CLEO's one due to the effective BG rejection and increase of the data sample and achieves at the level that limits the parameter-space of NP models such as minimal SUSY + seesaw mechanism. In addition, a search for $B^0 \rightarrow \ell\tau$, $B \rightarrow K\mu\tau$ and $\Upsilon(nS) \rightarrow \mu\tau$ is also performed.

Hopefully, in the near future, we will learn from complementary studies at LHC and super B -factories what NP is.

Table 3. List for the current upper limits for τ LFV decays with the analyzed luminosity at BaBar, Belle and CLEO. Here, the symbols mean that $\ell=e$ or μ , $P^0 = \eta, \eta'$, or π^0 , $h = \pi$ or K and $V^0 = \rho^0, K^*, \bar{K}^{*0}$, or ϕ . The Belle's result for $\tau \rightarrow h + \Lambda/\bar{\Lambda}$ does not include $K\Lambda$ and $K\bar{\Lambda}$. For $\tau \rightarrow \ell f_0(980)$, the upper limits are given for the product $\mathcal{B}(\tau \rightarrow \ell f_0(980)) \times \mathcal{B}(f_0 \rightarrow \pi\pi)$.

	BaBar		Belle		CLEO
	$\mathcal{B}(\times 10^{-8})$	Lum.(fb $^{-1}$)	$\mathcal{B}(\times 10^{-8})$	Lum.(fb $^{-1}$)	$\mathcal{B}(\times 10^{-8})$
$\tau \rightarrow \mu/e + \gamma$	6.8/11	252	4.5/12	535	110/270
$\tau \rightarrow \ell + P^0$	11–16	339	7–12	401	370–960
$\tau \rightarrow \mu/e + K_s^0$	4.0/3.3	469	4.8/5.6	282	95/91
$\tau \rightarrow \ell + \ell' + \ell''$	3.7–8.0	376	2.0–4.1	535	150–290
$\tau \rightarrow \ell + h' + h''$	7.0–48	221	20–160	158	190–820
$\tau \rightarrow \ell + V^0$	0.8–18	451	5.9–13	543	200–750
$\tau \rightarrow \mu/e + \omega$	10/11	384	8.0/18	543	—
$\tau \rightarrow h + \Lambda/\bar{\Lambda}$	5.8–15	237	7.2–14	154	—
$\tau \rightarrow \ell f_0(980)$	—	—	3.2 – 3.4	671	—

References

- [1] X. Y. Pham, Eur. Phys. J. C **8**, 513 (1999).
- [2] G. Cvetič, C. Dib, C. S. Kim and J. D. Kim, Phys. Rev. D **66**, 034008 (2002) [Erratum-ibid. D **68**, 059901 (2003)].
- [3] C. X. Yue, Y. m. Zhang and L. j. Liu, Phys. Lett. B **547**, 252 (2002).
- [4] T. Fukuyama, T. Kikuchi and N. Okada, Phys. Rev. D **68**, 033012 (2003).
- [5] J. R. Ellis, J. Hisano, M. Raidal and Y. Shimizu, Phys. Rev. D **66**, 115013 (2002).
- [6] A. Brignole and A. Rossi, Phys. Lett. B **566**, 217 (2003).
- [7] M. Sher, Phys. Rev. D **66**, 057301 (2002).
- [8] E. Arganda, M. J. Herrero and A. M. Teixeira, versus JHEP **0710**, 104 (2007), E. Arganda, M. J. Herrero and J. Portoles, MSSM-seesaw JHEP **0806**, 079 (2008).
- [9] C. x. Yue, Y. m. Zhang and L. j. Liu, Phys. Lett. B **547**, 252 (2002), M. Blanke, A. J. Buras, B. Duling, A. Poschenrieder and C. Tarantino, Higgs JHEP **0705**, 013 (2007).
- [10] A. Abashian *et al.* (Belle Collaboration), Nucl. Instr. and Meth. A **479**, 117 (2002).
- [11] S. Kurokawa and E. Kikutani, Nucl. Instr. and Meth. A **499**, 1 (2003), and other papers included in this Volume.
- [12] B. Aubert *et al.* [BABAR Collaboration], Nucl. Instrum. Meth. A **479**, 1 (2002).
- [13] G. J. Feldman and R. D. Cousins, Phys. Rev. D **57**, 3873 (1998).
- [14] I. V. Narsky, Nucl. Instr. Meth. A **450**, 444 (2000).
- [15] K. Hayasaka *et al.* (Belle Collaboration), Phys. Lett. B **666**, 18 (2008).
- [16] B. Aubert *et al.* (BABAR Collaboration), Phys. Rev. Lett. **95**, 041802 (2005).
- [17] B. Aubert *et al.* (BABAR Collaboration), Phys. Rev. Lett. **96**, 041801 (2006).
- [18] Y. Miyazaki *et al.* (Belle Collaboration), Phys. Lett. B **648**, 341 (2007).
- [19] B. Aubert *et al.* (BABAR Collaboration), Phys. Rev. Lett. **98**, 061803 (2007).

- [20] Y. Miyazaki *et al.* (Belle Collaboration), Phys. Lett. B **660**, 154 (2008).
- [21] B. Aubert *et al.* (BABAR Collaboration), Phys. Rev. Lett. **99**, 251803 (2007).
- [22] Y. Miyazaki *et al.* (Belle Collaboration), Phys. Lett. B **672**, 317 (2009).
- [23] N. Nishio *et al.* (Belle Collaboration), Phys. Lett. B **664**, 35 (2008).
- [24] B. Aubert *et al.* (BABAR Collaboration), Phys. Rev. Lett. **100**, 071802 (2008).
- [25] M. Roney's slide shown at TAU08. See <http://tau08.inp.nsk.su/>.
- [26] B. Aubert *et al.* (BABAR Collaboration), Phys. Rev. D **77**, 032007 (2008).
- [27] B. Aubert *et al.* (BABAR Collaboration), Phys. Rev. D **77**, 091104(R) (2008).
- [28] B. Aubert *et al.* (BABAR Collaboration), Phys. Rev. Lett. **99**, 201801 (2007).
- [29] W. Love *et al.* (CLEO Collaboration), Phys. Rev. Lett. **101**, 201601 (2008).